This is a peer-reviewed, author's accepted manuscript of the following research article:
Bao, H., Shen, J., Peng, H., Liu, Y., & Chen, H. (2023). Elastic core concept for modified Bree problems considering in-phase and out-of-phase loading conditions. International Journal of Pressure Vessels and Piping, 202, [104913].
https://doi.org/10.1016/j.ijpvp.2023.104913

Elastic core concept for modified Bree problems considering in-phase and out-of-phase loading conditions

Hongchen Bao[1, 2], Jun Shen[3], Heng Peng[1], Yinghua Liu[2*], Haofeng Chen[4*, 5]

1. Institute of Nuclear and New Energy Technology, Tsinghua University, Beijing, 100084, China
2. Department of Engineering Mechanics, AML, Tsinghua University, Beijing, 100084, China
3. School of Energy and Power Engineering, University of Shanghai for Science and Technology, Shanghai, China
4. Key Laboratory of Pressure Systems and Safety (DOE), School of Mechanical and Power Engineering, East China University of Science and Technology, Shanghai, 200237, China
5. Department of Mechanical and Aerospace Engineering, University of Strathclyde, 75 Montrose Street, Glasgow G1 1XJ, Scotland, United Kingdom

Abstract: The elastic core concept developed from the Bree problem can be used for structural integrity evaluation of high temperature components, such as creep ratcheting and creep fatigue. The simplified inelastic analysis method of the ASME 2013 III-1 NH Code adopts the idea of core stress, which protects against creep rupture and collapse of the structure by limiting the accumulated inelastic strain. Currently, the formulas of core stress and evaluation diagram of effective creep stress parameter for Tests B-1 and B-3 adopted by the APPENDIX NH-T are developed from the classical loading Bree problem, however, the related concepts and evaluation diagrams of modified Bree problems considering generalized loading conditions have not been reported. This paper first reviews the development history of the elastic core concept and its corresponding analysis methods. Based on the modified Bree problems considering in-phase and out-of-phase loading developed by Bradford, the corresponding formulas of the core stress in the non-plastic ratcheting zone are completely proposed, and the corresponding evaluation diagrams of effective creep stress parameters are constructed for the first time. By comparing the core stress formulas and effective creep stress parameter diagrams under three loading cases, the conservatism and applicability of the classical core stress method are discussed. In addition, the differences and relations between two creep ratcheting assessment methods applicable to transient and sustained thermal load conditions respectively are clarified. The new results and conclusions presented in this paper can deepen the understanding of structural response under complex loading conditions, and provide guidance for shakedown analysis and creep ratcheting assessment of high-temperature components.

Keywords: Elastic core; In-phase loading; Out-of-phase loading; Bree problem; Creep ratcheting

*Corresponding author email: [2] yhliu@tsinghua.edu.cn (Y. Liu), [4] haofeng.chen@ecust.edu.cn (H. Chen).

1 Introduction

The concept of elastic core refers to the portion of the wall section that remains elastic state during the whole cyclic thermal-mechanical loading history of the structure. The core stress in elastic core can be used for creep ratcheting assessment, which is a very effective simplified analysis method for structural design and integrity evaluation in engineering[1-3]. At present, the core stress method has been adopted in the international mainstream design codes for high-temperature structures, such as the ASME III NH code[4] and the assessment method for cyclically enhanced creep in the R5 procedure[5].The elastic core concept originates from the Bree problem that is usually applicable to axisymmetric thin-walled cylindrical shell structures, however, the core stress method can be applied to any type of structure and loading cases. Therefore, this method is of great significance to the shakedown analysis and structural integrity evaluation of high-temperature structures.

In the 1970s, O 'Donnell and Porowski[2] proposed the concept of elastic core and derived the core stress formulas, and presented a modified Bree diagram containing equal core stress lines (i.e. effective creep stress parameter diagram) in the non-plastic ratcheting region. Combined with the isochronous stress-strain curve, the equal core stress lines are actually the equal life lines at a given upper bound of accumulated inelastic strain[2]. Therefore, the simplified inelastic analysis method based on effective creep stress parameter diagram and isochronous stress-strain curve diagram can greatly reduce the high cost of detailed inelastic analysis of creep ratcheting effects. In 1979, the concept of elastic core was extended from the non-plastic ratcheting region (E, S_1, S_2, P) to the ratcheting region (R_1, R_2) of the Bree diagram to include the plastic ratcheting regime[3]. The extended generalized core stress graph was adopted by the ASME code and is still in use till now. The extended elastic core concept can consider the effects of strain hardening, temperature dependence of yield stress, and the effects of severe cycles resulting in plastic ratcheting[3]. Later, the generalized core stress graph was extended to determine the upper bound of inelastic strain range for fatigue damage and the upper bound of maximum residual stress for creep rupture damage[6]. In 1981, the core stress graph derived from the uniaxial model was extended to consider the arbitrary biaxiality of primary membrane and thermal bending respectively[7]. However, the biaxial model was not widely used in engineering. The effective creep stress parameter diagram developed by O 'Donnell and Porowski was used in Tests B-1 and B-3 of the ASME III NH-T code, where Test B-1 is applicable to structures with negligible peak stress, and Test B-3 applies to axisymmetric structure and loading[8]. In 1989, Sartory[9] proposed another effective creep stress parameter diagram considering the effect of peak strain. The new revised diagram is more conservative and can be applied to any structure and loading. The modified diagram given by Sartory has also been adopted by the ASME code and has been used ever since, which is applicable to Test B-2. However, the code does not explicitly give the effective creep stress parameter formula of Sartory's diagram.

In 2006, McGreevy [10] studied the influence of temperature-dependent yield strength on the evolution of core stress. The core stress, primary and secondary stresses were normalized by the yield strength at the hot end, which is different from the dimensionless treatment with the cold end yield strength commonly used in ASME codes and literatures. In 2014, Bradford[11] completely derived the modified Bree problems with different yield stresses during on-load and off-load under

the conditions of classical Bree loading and in-phase loading. Based on the derived creep ratchet strain and the creep ductility of the material, Bradford proposed another creep ratcheting assessment method (creep ductility exhaustion approach) different from the core stress method. The classical core stress method assumes that the cyclic thermal gradient on the wall thickness is a transient condition, and the core stress usually corresponds to the steady operation phase after the removal of the transient temperature gradient. However, Bradford's new assessment method is applicable to the situation where there is a sustained thermal gradient during the steady on-load operation.

In addition to the simplified inelastic analysis method for high temperature components, the elastic core is also an elastic-plastic ratcheting assessment method as adopted by ASME VIII-2[12]. For the Bree problem, the existence of elastic core means that plastic ratcheting will not occur. According to the research of Kalnins[13, 14], the elastic core criterion used as ratcheting assessment applicable to any geometry and loading. For the classical Bree problem, the elastic core remains unchanged after the first cycle. However, for practical structural problems, the elastic core may shrink as the number of cycles increases. Usually, the elastic core still exists after the agreed number of cycles is a practical ratcheting check method[14]. For the shakedown problem of actual complex structures, it is possible that ratcheting has occurred but there is still an elastic core at the corners or junctions[1]. Therefore, the elastic core criterion needs to check the primary-load-bearing boundary.

Although the elastic core method has wide applicability, it still has many limitations. Firstly, the core stress is derived from the uniaxial beam model, and the application to arbitrary structures inevitably leads to conservative or non-conservative problems. Generally, the code method is conservative, but it may be too conservative. In some special cases, the code method may also be non-conservative, which requires continuous investigation and revision by scholars and engineers. Secondly, the effective creep stress parameter diagram developed by O'Donnell and Porowski [2,3] is based on the classical Bree loading. Although the modified diagram given by Sartory[9] can be applied to any loading, this extended application is actually established based on the verification of typical cases. Sartory's modified diagram is more conservative than O'Donnell-Porowski method, and Sartory only modified the temperature profile compared to the O'Donnell-Porowski method, but did not modify the loading condition. In fact, the modified Bree problem considering the influence of different loading conditions has gained wide developments in the past decades, such as the in-phase loading problem [15], out-of-phase loading problem [16], and generalized loading problem [17]. However, to the best of the authors' knowledge, the effective creep stress parameter diagrams similar to O'Donnell-Porowski method corresponding to these modified Bree problems have not been established. Thirdly, the two effective creep stress parameter diagrams given in the code are both obtained based on the uniaxial two-stress parameters Bree problem. However, the shakedown analysis and design method based on stress classification usually considers multiple stress parameters. In fact, the code extends the meaning of the coordinate axes of the O'Donnell-Porowski and Sartory assessment diagrams. Therefore, the code method actually extends the two-stress parameters problem to the multi-stress parameters problem, and uses the uniaxial problem to approximate the multi-axis problem. The mismatch between the simplified assessment method and the actual situation will lead to conservative or non-conservative problems. Currently, some progress has been made in the modified Bree problems considering the effects of multiple stress parameters, such as the work of Reinhardt[18], Adibi-Asl[19], Shen[20], Bao[21,22], etc. The development of a multi-dimensional effective creep stress parameter diagram is worthy of further

study.

The aim of this paper is to propose the effective creep stress parameter diagrams and core stress formulas of the modified loading Bree problems based on O'Donnell and Porowski method and Bradford's research, and to reveal two creep ratcheting assessment methods under different thermal load conditions. Section 2 reviews the elastic core concept of classical Bree problem, so as to compare with the elastic core characteristics of modified loading Bree problems. In Section 3 and Section 4, the elastic core concepts for modified loading Bree problems are discussed, and the corresponding core stress formulas and effective creep stress parameter diagrams are established respectively. In Section 5, the effective creep stress parameter diagrams for three types of loading conditions are compared and discussed, and the similarities and differences of two kinds of creep ratcheting assessment methods under different thermal load conditions are clarified. Section 6 summarizes the conclusions of this paper.

2. Elastic core concept of classical Bree problem

The classical Bree problem is a uniaxial ratcheting problem, which is a simplified analytical model of axisymmetric thin-walled cylindrical shell structure subjected to constant internal pressure and cyclic linear temperature gradient on the wall thickness. The core stress is actually a characteristic stress of the steady-state stress cycle of the Bree problem, so all the basic assumptions adopted by the Bree problem are followed, such as the plane section assumption, the elastic-perfectly plastic material assumption, without strain hardening assumption, and temperature independence assumption of material parameters, etc. In the start-up and shutdown initial stages of pressure vessels, transient thermal gradients can cause thermal bending stress. In the steady-state of equipment operation and a period of time after shutdown, the temperature on the structure wall thickness reaches uniform, that is, the temperature gradient is removed and the thermal bending stress disappears. The core stress corresponds to the high-temperature steady operation stage after the temperature gradient has been removed. When the stress tends to relax, the creep strain gradually accumulates. The creep strain is assumed to be negligible at the low-temperature shutdown stage. Therefore, the core stress is the key information for bounding the inelastic strain caused by creep. By limiting the maximum inelastic strain in the whole elastic core, the creep ratcheting strain at any point on the section during the whole cyclic loading process can be bounded, that is, the maximum core stress corresponds to the lowest upper bound of the accumulated creep ratcheting strain.

The effective creep stress parameter diagram of the classical Bree problem is shown in Fig.1, which is used for Test B-1 in the ASME III NH-T code. The abscissa in Fig.1 is the dimensionless constant primary membrane stress $X=\sigma_p/S_{yL}$, the ordinate is the dimensionless cyclic thermal bending stress range $Y=\Delta\sigma_b/S_{yL}$, $Z=\sigma_c/S_{yL}$ is the dimensionless core stress, also known as the effective creep stress parameter. S_{yL} denotes the yield strength at mean temperature of cold end. In Fig.1, Zone E (pure elasticity), Zone S_1 and S_2 (elastic shakedown), and Zone P (plastic shakedown) represent different elastic-plastic behaviors under different stress combinations. The border lines between regions and equal Z-value lines are derived through the uniaxial rectangular section beam. The characteristic stress distributions of different elastic-plastic behaviors under steady-state cycle are shown in Fig.2.

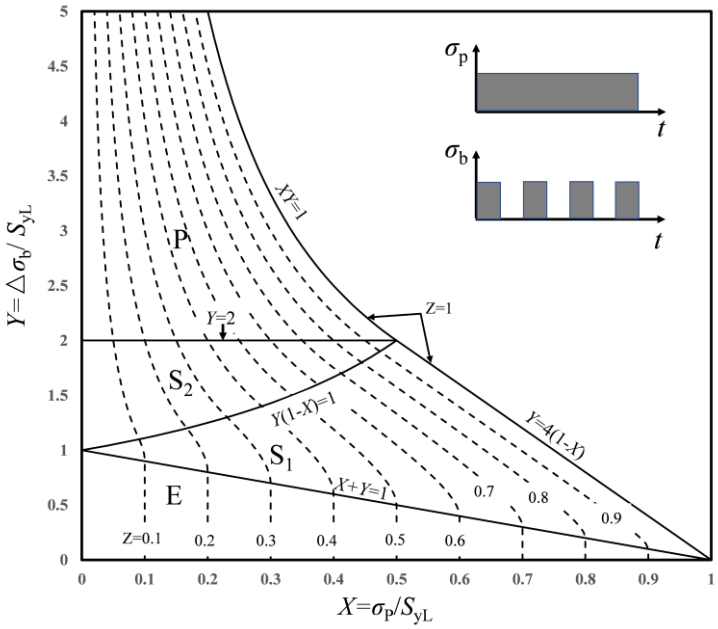

Fig.1. Effective creep stress parameter diagram of classical Bree problem (adopted by ASME III NH)

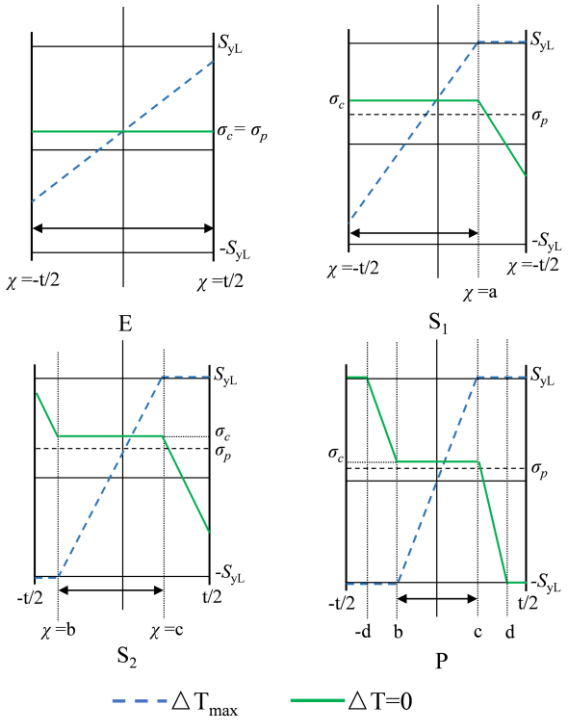

Fig.2. Steady-state cyclic stress distribution of Bree problem

The stepwise derivation of the Bree problem utilizes two basic principles, namely the equilibrium condition of force (Eq.(1)) and the additive decomposition of strain (Eq.(2)), as shown below. t is the section thickness in Eq.(1). The total strain ε in Eq.(2) is composed of elastic strain ε_e, plastic strain ε_p, and the thermal strain ε_{th}. E is the modulus of elasticity. ΔT is the linear temperature gradient between the inner and outer walls of the section, and cycles between a maximum value and zero with the startup and shutdown of the equipment.

$$\int_{-t/2}^{+t/2} \sigma \cdot d\chi = t\sigma_p \tag{1}$$

$$\varepsilon = \varepsilon_e + \varepsilon_p + \varepsilon_{th} = \begin{cases} \dfrac{\sigma}{E} + \varepsilon_p - \dfrac{2\sigma_b}{Et}\chi, \Delta T = \Delta T_{\max} \\ \dfrac{\sigma}{E} + \varepsilon_p, \Delta T = 0 \end{cases} \tag{2}$$

The two types of stresses considered in the Bree problem correspond to the hoop direction of the axisymmetric shell, and the total strain ε on the section is independent of χ , that is, the uniaxial beam model cannot rotate, so the characteristics of the stress distributions can be determined according to the stress-strain relationship Eq.(2). For example, when $\Delta T = \Delta T_{\max}$, then $\frac{\sigma}{E} + \varepsilon_p = \frac{2\sigma_b}{Et}\chi + C$, where C is a constant value. When the slope of ε_p with respect to χ is $\frac{2\sigma_b}{Et}$, the slope of σ with respect to χ is zero, and vice versa. Combined with the equilibrium condition on the whole section of each cycle, the coordinates of the elastic-plastic interface (a, b, c, d) under various stress distributions can be obtained as follows:

$$a = -\frac{1}{2}t(1 - 2\sqrt{\frac{1-X}{Y}}) \tag{3}$$

$$b = -\frac{1}{2}t(X + \frac{1}{Y}) \tag{4}$$

$$c = \frac{1}{2}t(\frac{1}{Y} - X) \tag{5}$$

$$d = \frac{t}{Y} \tag{6}$$

The blue dotted lines in Fig. 2 show the stress distributions with maximum transient temperature gradients ΔT_{max} and constant mechanical loads under steady-state cycles, and corresponding to the initial stages of equipment startup and shutdown. The solid green lines show the stress distributions when the temperatures are uniform across the wall thickness, i.e. the temperature gradient ΔT is zero, such as during the steady operation stage and after a period following shutdown. According to the definition of elastic core, the width marked by the two-way arrows in Fig. 2 is the the elastic core under various elastic-plastic behaviors. For example, for pure elastic behavior (E), the entire wall thickness is elastic core. When ΔT =0, the maximum stress in the elastic core is the core stress σ_c. For Bree problem, the core stress is a plateau value. The core stress can be derived from elastoplastic interface coordinates and equilibrium conditions under different behaviors. According to the literature [2], the dimensionless core stress formulas can be given by Eqs.(7) - (9), which are also the effective creep stress parameters given by the ASME III NH code. Among them, Eq.(7) is applicable to S_2 and P zones, Eq.(8) is applicable to S_1 zone, and Eq. (9) is applicable to E zone.

$$Z = XY, \quad for\ \mathrm{S_2}\ \text{and P regimes} \tag{7}$$

$$Z = Y + 1 - 2\sqrt{(1-X)Y}\ , for\ \mathrm{S_1}\ \text{regime} \tag{8}$$

$$Z = X, for\ \text{E regime} \tag{9}$$

3. Elastic core concept of modified Bree problem considering in-phase loading

The in-phase loading condition refers to the proportional variation of mechanical load and thermal load. Moreton and Ng [23-25] published a series of articles in the 1980s on the modified Bree problems considering in-phase and out-of-phase loading conditions, and had given the corresponding ratchet boundaries and plastic strains for the two types of problems. However, there were some oversights in the derivation of their original paper, and the subsequent correcting papers did not receive much attention[26]. In recent years, Bradford[15,16] independently rederived the in-phase and out-of-phase loading Bree problems, and gave complete solutions to the two types of problems (including shakedown and ratcheting boundaries, stress and strain distributions, and geometric parameters, etc.). Considering that Bree problem has been the basis of ratcheting assessment in many codes for decades, Bradford's extension work has important theoretical value and engineering significance. In this section, the effective creep stress parameter diagram similar to O 'Donnell and Porowski method is developed on the basis of the modified Bree problem considering in-phase loading condition, so as to provide reference and guidance for shakedown design and creep ratcheting evaluation of elevated temperature structures.

The modified Bree diagram under in-phase loading condition given by NG [24] and Bradford [15] is shown in Fig.3, where E represents pure elastic behavior, S_1 and S_2 represent two types of elastic shakedown, and P_1, P_2 , P_3 represent different plastic shakedown behaviors. Note that the abscissa of Fig. 3 is the dimensionless primary membrane stress range $\Delta X = \Delta\sigma_p / S_{yL}$, which is different from that of Fig. 1. For the in-phase loading modified Bree problem, the force equilibrium conditions are different with and without temperature gradients, as shown in Eq. (10), and the principle of additive decomposition of strain and the assumption of no bending of section remain the same as for the original Bree problem.

$$\int_{-t/2}^{+t/2} \sigma \cdot d\chi = \begin{cases} t\sigma_p, \Delta T = \Delta T_{\max} \\ 0, \Delta T = 0 \end{cases} \tag{10}$$

Fig. 4 shows the steady-state stress cycles for different elastoplastic behaviors of the in-phase loading modified Bree problem. The black dotted lines represent the stress distributions when the primary load and temperature gradient are simultaneously applied, and the red solid lines represent the stress distributions after the primary load and temperature gradient are simultaneously removed. Note that the temperature gradient here is still assumed to be a transient condition, and the temperature dependence of yield strength is not considered.

Similar to the elastic core concept of the classic Bree problem, the width marked by the bidirectional arrows in Fig. 4 is the elastic core, the stress in the red solid line platform in the elastic core area is the core stress σ_c. According to stress distribution characteristics and force equilibrium condition, the coordinates of the elastic-plastic interfaces in Fig. 4 can be obtained, as shown in Eqs (11)-(16), where Eqs (11) to (13) have the same form as Eqs (3) to (5), but X needs to be replaced by ΔX .

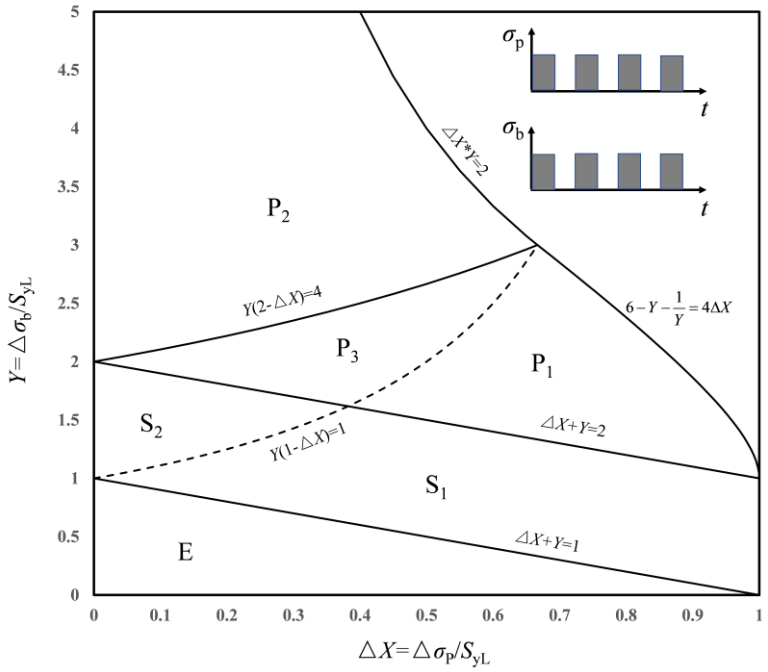

Fig.3. Modified Bree diagram under in-phase loading

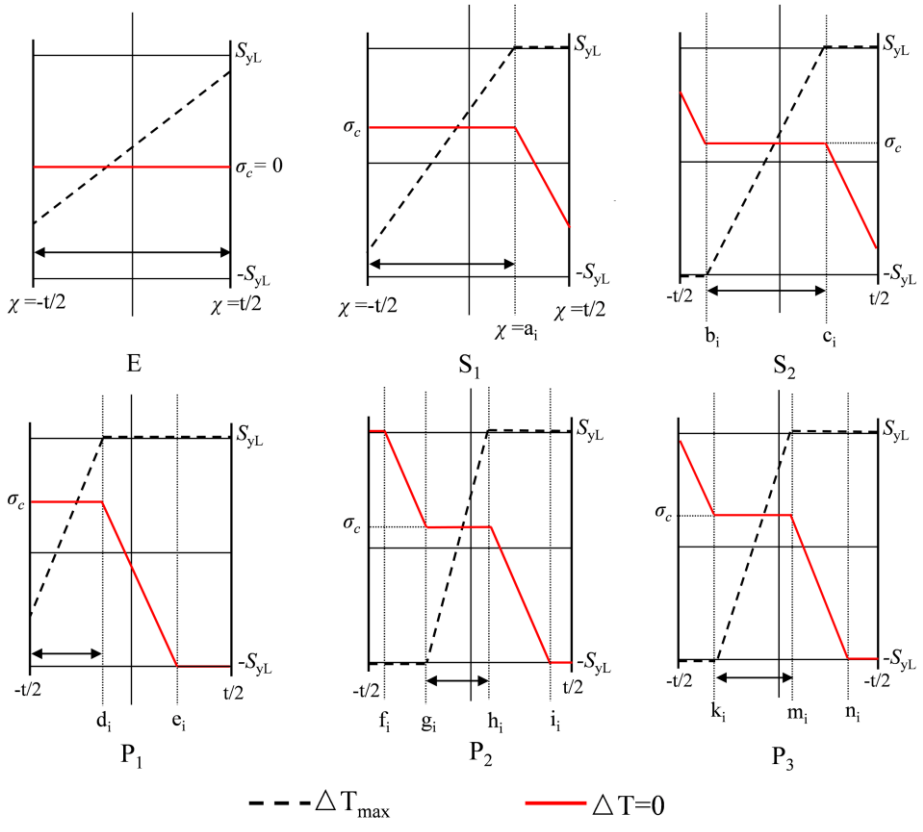

Fig.4. Steady-state stress cycle of in-phase loading Bree problem

$$a_i = d_i = -\frac{1}{2}t(1-2\sqrt{\frac{1-\Delta X}{Y}}) \tag{11}$$

$$b_i = g_i = k_i = -\frac{1}{2}t(\Delta X + \frac{1}{Y}) \tag{12}$$

$$c_i = h_i = m_i = \frac{1}{2}t(\frac{1}{Y} - \Delta X) \tag{13}$$

$$e_i = n_i = \frac{1}{2}t(2\sqrt{\frac{2-\Delta X}{Y}} - 1) \tag{14}$$

$$f_i = -\frac{1}{2}t(\frac{2}{Y} + \frac{\Delta X}{2}) \tag{15}$$

$$i_i = \frac{1}{2}t(\frac{2}{Y} - \frac{\Delta X}{2}) \tag{16}$$

The effective creep stress parameters for different regimes can also be obtained according to the elastic-plastic interface coordinates and equilibrium conditions, as shown in Eqs. (17)-(22). Eqs. (18) - (22) are some characteristic stresses of the in-phase loading Bree problem obtained in literature[15], however, the concept of effective creep stress has not been difined. In fact, literature[15] also marked the elastic core of the in-phase loading Bree problem. However, the elastic core marked in literature[15] is different from the concept of elastic core defined in this paper. For example, for the P_2 regime in Fig. 4, the elastic core marked in the literature[15] is f_ii_i, while the elastic core marked in this paper is g_ih_i. The elastic core given in the literature[15] corresponds to the section width that remains elastic cycling after the first half-cycle. (The cycle here refers to the steady-state stress cycle, that is, the third half-cycle is consistent with the first half-cycle, and so on. The black dotted line in Fig.4 corresponds to the first half-cycle, the red solid line corresponds to the second half-cycle.) However, the elastic core definition given in this paper corresponds to the section width that has always been in the elastic state throughout the cyclic loading history, that is, the stress has never reached yield and the plastic strain remains zero. The inelastic strain in the elastic core only includes the creep strain. By comparison, the elastic core definition in this paper is consistent with O'Donnell and Porowski method and the definition in the literature [1, 26]. Therefore, this section defines the elastic core concept and effective creep stress of the in-phase loading Bree problem based on the classical concept of elastic core and Bradford's results.

$$Z = 0\,, \quad for \text{ E regime} \tag{17}$$

$$Z = (\sqrt{Y} - \sqrt{1-\Delta X})^2\,, \quad for \ S_1 \text{ regime} \tag{18}$$

$$Z = \Delta X(Y-1)\,, \quad for \ S_2 \text{ regime} \tag{19}$$

$$Z = 2\sqrt{Y}(\sqrt{(2-\Delta X)} - \sqrt{(1-\Delta X)}) - 1\,, \quad for \ P_1 \text{ regime} \tag{20}$$

$$Z = \frac{\Delta X}{2}Y\,, \quad for \ P_2 \text{ regime} \tag{21}$$

$$Z = 2\sqrt{Y(2-\Delta X)} - Y(1-\Delta X) - 2\,, \quad for \ P_3 \text{ regime} \tag{22}$$

According to Eqs. (17) to (22), the effective creep stress parameter diagram of the in-phase loading Bree problem can be constructed, as shown in Fig. 5. It can be seen that the distributions of equal Z-value lines are significantly different from that of the original Bree problem. For zone E with pure elastic behavior, when the thermal gradient is removed, the mechanical load is removed simultaneously, so the whole thickness is the elastic core, and the core stress in the E zone is zero. For Eq. (18), when Z=0, the boundary $\Delta X + Y = 1$ between zone E and zone S_1 can be obtained. For the two types of elastic shakedown behaviors (S_1 and S_2), although the steady-state stress distributions and the elastic-plastic interface coordinates of the in-phase loading Bree problem are similar to those of the classical Bree problem, the effective creep stresses are different due to the different equilibrium conditions after temperature gradient removal under the two types of loading. From Eqs. (18) to (22), it can be seen that the core stress formulas of plastic shakedown zones are different from those of elastic shakedown zones, while for classical Bree problem, the core stress formulas of S_2 zone and P zone are the same. When Z=1, that is, when the core stress is equal to the yield strength S_{yL}, Eqs. (20) to (22) are exactly equivalent to the ratcheting boundary in Fig. 3. Z=1 means that the elastic core on the section disappears, and the whole section will reach yield during the load cycle.

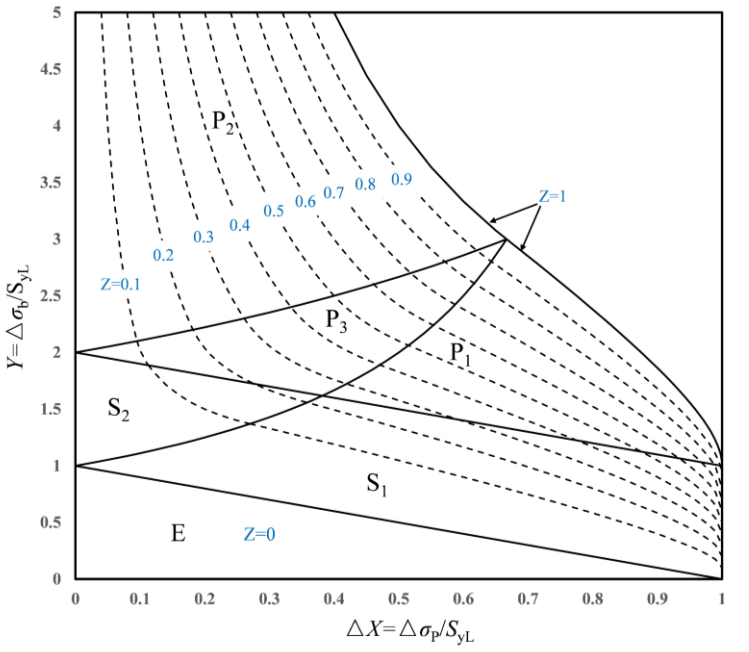

Fig.5. Effective creep stress parameter diagram for in-phase loading modified Bree problem

In order to verify the elastic-plastic interface coordinates given by Eqs. (11-16) and the effective creep stress parameters given by Eqs. (18-22), the above theoretical solutions and numerical solutions based on the finite element step-by-step analysis are compared. The common two-plane model proposed by the authors[22] for uniaxial Bree-type problems is adopted for numerical analysis, as shown in Fig.6. The upper plane and lower plane are rigidly coupled in direction-2, and the stress sections are not allowed to rotate. Only in-phase mechanical membrane stress (controlled by F) and thermal bending stress (controlled by the temperature gradient 2T) are applied to the model. The element type is CPS8 in ABAQUS and the material property is ideal

elastoplastic. The material parameters are: Young's modulus E=200Gpa, Poisson's ratio ν=0.3, Yield stress S_{yL}=300Mpa, Coefficient of thermal expansion α=1E-5 $\circ C^{-1}$. The strain hardening and temperature-dependent effect are not considered. The von-Mises yield condition and associated plasticity rule are adopted, as well as the small displacement theory. A uniform and fine mesh is used to accurately obtain the stress distribution on the entire section.

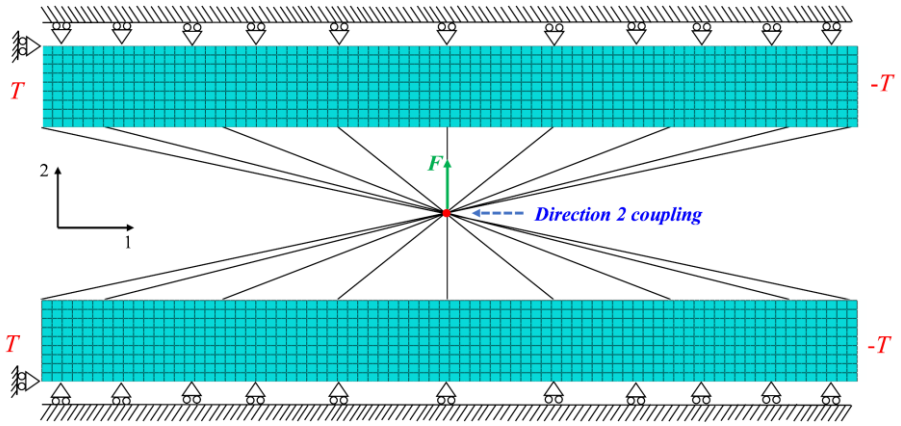

Fig.6. Two-plane model used for the determination of elastic core

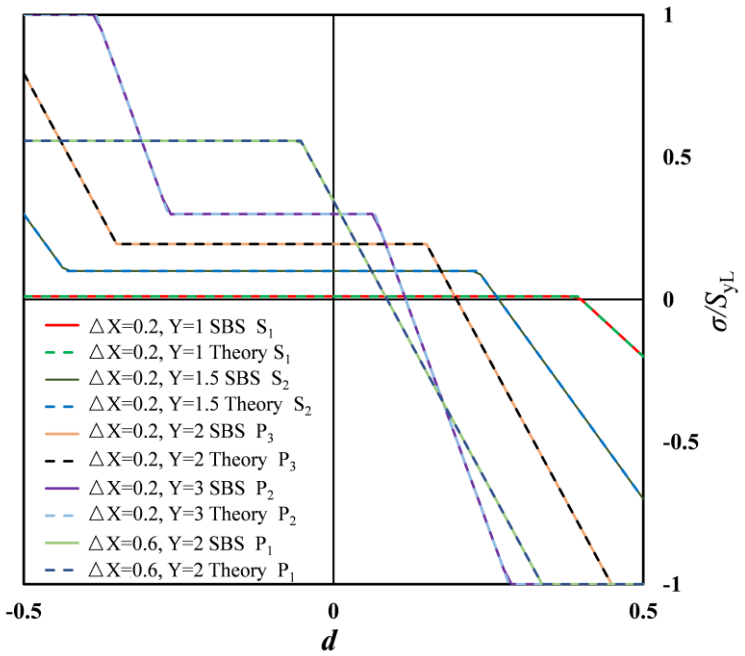

Fig.7. Comparison of numerical and theoretical solutions for elastic core of the in-phase loading Bree problem

In Fig. 7, some typical load combinations are selected to compare the corresponding numerical and theoretical solutions of elastic cores. The solid lines of various colors correspond to the stress distributions after the removal of the temperature gradients (ΔT=0) obtained by numerical analysis. The dotted lines in Fig. 7 are the stress distributions directly constructed according to Eqs. (11) to (22), corresponding to the state of red lines in Fig. 4. For all elastoplastic behaviors, the numerical and theoretical solutions of the elastic core agree well, which proves the correctness of the

coordinates of the elastoplastic interface and the effective creep stress parameters given above.

4. Elastic core concept of Bree problem considering out-of-phase loading

The out-of-phase loading Bree problem refers to the cyclic mechanical and thermal loads are not synchronous and with a phase shift. When the mechanical and thermal loads stagger exactly a complete phase cycle, it is also called anti-phase loading. The problem analyzed in this section is based on the out-of-phase loading Bree problem derived by Bradford[16], using the so-called "positive-phase load sequence", that is, a complete loading cycle consists of four load states. The first load state has both the maximum thermal gradient and mechanical load; The second load state only applies mechanical load, and the thermal gradient is removed; The mechanical load and thermal gradient at the third load state are both removed, and the thermal gradient at the fourth load state is reapplied; The mechanical load is reapplied at the fifth load state, returning to the first load state, and then the repeated load cycles continue. The modified Bree diagram under out-of-phase loading is shown in Fig. 8. Note that the boundaries indicated by arrows are obtained by numerical solution based on complex parametric equations.

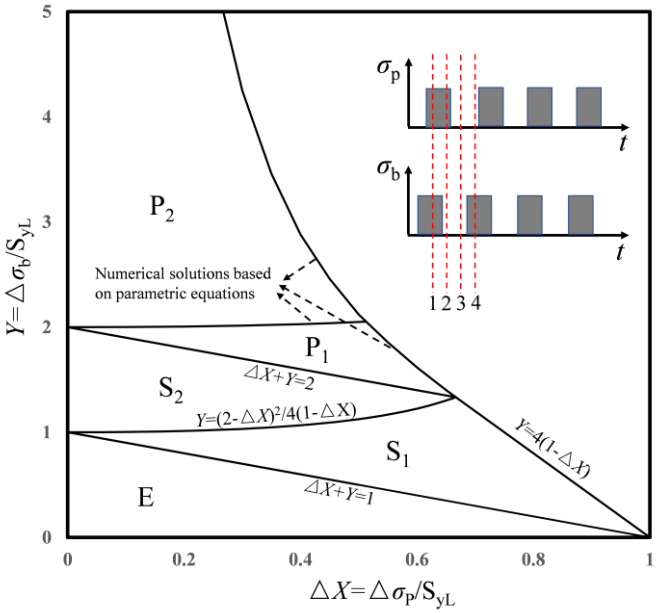

Fig.8. Modified Bree diagram under positive out-of-phase loading condition

For the out-of-phase loading modified Bree problem, the principle of additive decomposition of strain is still given by Eq. (2), while the force equilibrium can be given by Eq. (23).

$$\int_{-t/2}^{+t/2} \sigma \cdot d\chi = \begin{cases} t\sigma_p, P = P_{\max} \\ 0, P = 0 \end{cases} \tag{23}$$

Fig. 9 shows the steady-state stress distributions of five different elastic-plastic behaviors of the out-of-phase loading modified Bree problem. The coordinates of the elastic-plastic interface can still be derived from Eq.(2) and Eq.(23). For elastic shakedown behaviors S_1 and S_2, according to

the literature[16], the coordinates are given by Eqs. (24-26).

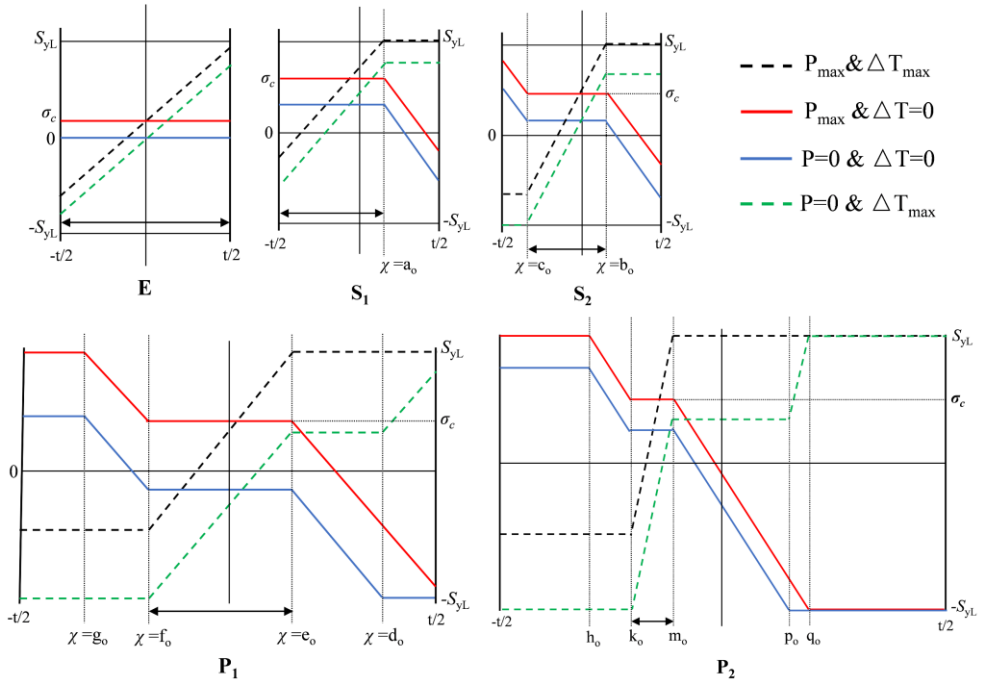

Fig.9. Steady-state stress cycle for the out-of-phase loading Bree problem

$$a_o = -\frac{1}{2}t(1-2\sqrt{\frac{1-\Delta X}{Y}}) \tag{24}$$

$$b_o = \frac{1}{2}t(\frac{2-\Delta X}{2Y}-\frac{\Delta X}{2-\Delta X}) \tag{25}$$

$$c_o = -\frac{1}{2}t(\frac{2-\Delta X}{2Y}+\frac{\Delta X}{2-\Delta X}) \tag{26}$$

For the two types of plastic shakedown behaviors P_1 and P_2, based on the equilibrium conditions of a complete cycle and the slope characteristics of the stress distributions, a series of simultaneous equations can be obtained, and then two sets of complex parametric equations can be derived to give their respective elastoplastic interface coordinates. The interface coordinates of P_1 regime are given by Eqs. (27-30), and those of P_2 regime are given by Eqs. (31-35). Eqs. (27-35) are derived for the first time in this paper. In Eqs. (27-35), $\bar{d}_o = d_o/t$, $\bar{g}_o = g_o/t$, $\bar{h}_o = h_o/t$, $\bar{p}_o = p_o/t$, $\bar{q}_o = q_o/t$, $\bar{f}_o = f_o/t$, $\bar{k}_o = k_o/t$。

$$d_o = t(\sqrt{(\bar{g}_o+\frac{1}{2})^2+\frac{2-\Delta X}{Y}}-\frac{1}{2}) \tag{27}$$

$$e_o = \frac{t}{2}\left[1-\frac{\bar{g}_o-\bar{g}_o^{\,2}-0.25+\frac{1-\Delta X}{Y}}{0.5(\bar{g}_o^{\,2}+\bar{g}_o-2\bar{d}_o+0.25)}-0.5(\bar{d}_o^{\,2}-\bar{d}_o+0.25+\frac{\Delta X-2}{Y})\right] \tag{28}$$

$$f_o = \frac{t}{2}\left[1-\frac{\bar{g}_o-\bar{g}_o^{\,2}-0.25+\frac{1-\Delta X}{Y}}{0.5(\bar{g}_o^{\,2}+\bar{g}_o-2\bar{d}_o+0.25)}+0.5(\bar{d}_o^{\,2}-\bar{d}_o+0.25+\frac{\Delta X-2}{Y})\right] \tag{29}$$

$$\left(\begin{array}{l} 23Y-32\Delta X+64\bar{g}_o^{\,2}Y+16\bar{g}_o^{\,3}Y+16\bar{g}_o^{\,4}Y-22Y\sqrt{4\bar{g}_o-4\frac{\Delta X}{Y}+4\bar{g}_o^{\,2}+\frac{8}{Y}+1}+44\bar{g}_oY \\ -8\bar{g}_oY\sqrt{4\bar{g}_o-4\frac{\Delta X}{Y}+4\bar{g}_o^{\,2}+\frac{8}{Y}+1}-24\bar{g}_o^{\,2}Y\sqrt{4\bar{g}_o-4\frac{\Delta X}{Y}+4\bar{g}_o^{\,2}+\frac{8}{Y}+1}+64 \end{array}\right)=0 \tag{30}$$

$$p_o = t\left(\sqrt{(\bar{h}_o+\frac{1}{2})^2+\frac{2-\Delta X}{Y}}-\frac{1}{2}\right) \tag{31}$$

$$q_o = \frac{1}{2}t(\bar{h}_o+\bar{p}_o+\frac{2}{Y}) \tag{32}$$

$$k_o = \frac{1}{2}t\left[2\bar{p}_o+\frac{(\bar{p}_o-\bar{q}_o)^2+\frac{2\bar{p}_o}{Y}}{\frac{1}{2}(\bar{h}_o-\bar{p}_o)}+\frac{1}{2}(\bar{h}_o-\bar{p}_o)\right] \tag{33}$$

$$m_o = \frac{1}{2}t\left[2\bar{p}_o+\frac{(\bar{p}_o-\bar{q}_o)^2+\frac{2\bar{p}_o}{Y}}{\frac{1}{2}(\bar{h}_o-\bar{p}_o)}-\frac{1}{2}(\bar{h}_o-\bar{p}_o)\right] \tag{34}$$

$$\left(\begin{array}{l} \bar{h}_o-0.25\Delta X-0.125Y-0.5\bar{h}_o^{\,2}Y-0.5\bar{h}_oY+\frac{1}{Y}+0.125Y\sqrt{4\bar{h}_o-\frac{4\Delta X}{Y}+4\bar{h}_o^{\,2}+\frac{8}{Y}+1} \\ +0.5\sqrt{4\bar{h}_o-\frac{4\Delta X}{Y}+4\bar{h}_o^{\,2}+\frac{8}{Y}+1}+0.25\bar{h}_oY\sqrt{4\bar{h}_o-\frac{4\Delta X}{Y}+4\bar{h}_o^{\,2}+\frac{8}{Y}+1}-1 \end{array}\right)=0 \tag{35}$$

The black dotted line in Fig. 9 corresponds to state 1 in Fig. 8, where the primary load P_{max} and the maximum temperature gradient ΔT_{max} act simultaneously; The red solid line corresponds to state 2 in Fig. 8, where ΔT_{max} is removed; The black solid line corresponds to state 3 in Fig. 8, where P_{max} is removed; The green dotted line corresponds to state 4 in Fig. 8, and the ΔT_{max} is reapplied. States 1 to 4 constitute a complete cycle and then repeats continuously. Note that the temperature gradient is still considered to be a transient condition and the temperature dependence of yield strength is not considered. In Fig. 9, the widths marked by the bidirectional arrows under various elastic-plastic behaviors are the corresponding elastic cores, and σ_c is the core stress. The core stress can be obtained according to the basic principles introduced above, as shown in Eqs. (36-40). It can be seen that Eqs. (36-37) are consistent with Eqs. (8-9) of the classical Bree problem, but it is need to replace X with ΔX.

$$Z = \Delta X, \quad \textit{for}\ \text{E regime} \tag{36}$$

$$Z = 1+Y-2\sqrt{Y(1-\Delta X)}, \quad \textit{for}\ S_1\ \text{regime} \tag{37}$$

$$Z = \frac{\Delta X}{2}+\frac{\Delta X}{2-\Delta X}Y, \quad \textit{for}\ S_2\ \text{regime} \tag{38}$$

$$Z = 1 - 2Y(\bar{f}_o - \bar{g}_o), \quad for\ \mathrm{P_1}\ \text{regime} \tag{39}$$

$$Z = 1 - 2Y(\bar{k}_o - \bar{h}_o), for\ \mathrm{P_2}\ \text{regime} \tag{40}$$

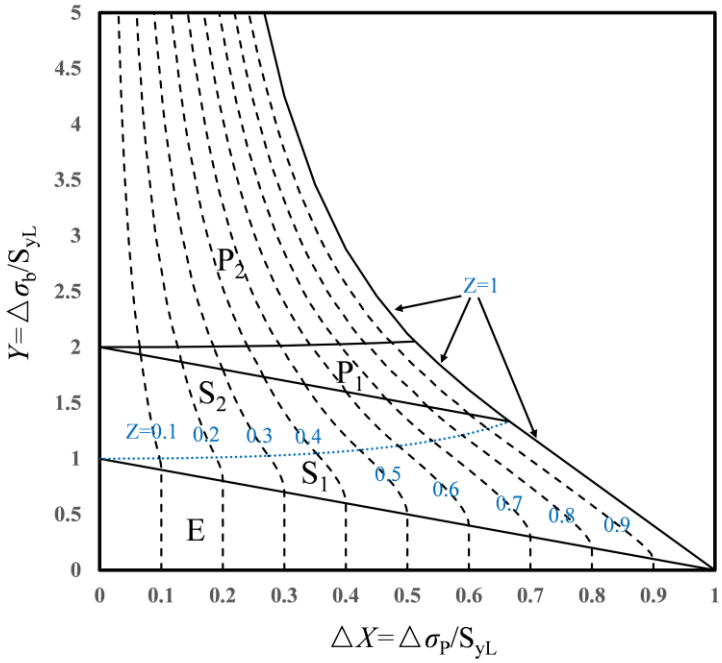

Fig.10. Effective creep stress parameter diagram for positive out-of-phase loading Bree problem

The effective creep stress parameter diagram under out-of-phase loading can be constructed according to formulas (36) to (40), as shown in Fig. 10. Note that the equal Z-value lines of P_1 and P_2 regions are obtained by numerical solutions of simultaneous parametric equations. For example, in P_1 region, when a set of coordinate values (ΔX,Y) are given, the parameter $\bar{g}_o$ can be obtained according to formula (30), and then parameters $\bar{d}_o$ and $\bar{f}_o$ can be obtained according to formulas (27) and (29), and then the corresponding core stress can be obtained based on formula (39). When Z=1, it can be verified that the equal Z-value line is consistent with the ratcheting boundary given in Fig. 8. The effective creep stress parameter diagram under out-of-phase loading is similar to that of the classical loading Bree problem, but significantly different from that of the in-phase loading Bree problem. Therefore, it is necessary to compare the effective creep stress parameter diagrams under three types of loading conditions, which will be discussed in the next section.

The numerical and theoretical solutions of elastic core under typical load combinations for the out-of-phase loading modified Bree problem are compared, as show in Fig. 11 and Fig. 12. The numerical solution is still obtained by the finite element step-by-step analysis of the two-plane model, and the analysis method is the same as that in the previous section. Fig. 11 shows that the numerical solutions of elastic core for S_1, S_2 and P_1 regimes agree well with the theoretical solutions, which proves the correctness of the proposed elastic-plastic interface coordinates and effective creep stress parameters. Fig. 12 shows that for P_2 regime, the numerical solution of the elastic core and

the theoretical solution can not be completely consistent, which is mainly due to the error of the numerical solution. The green and purple solid lines in Fig. 12 correspond to the 17th and 18th half cycles of the numerical solution, and the steady-state stress cycle has been reached at this time. The stress distribution characteristic of purple solid line shows that the numerical solution has obvious deviation in this situation. For P_2 regime, the numerical solution of the core stress is higher than the theoretical solution obtained from the above parametric equations.

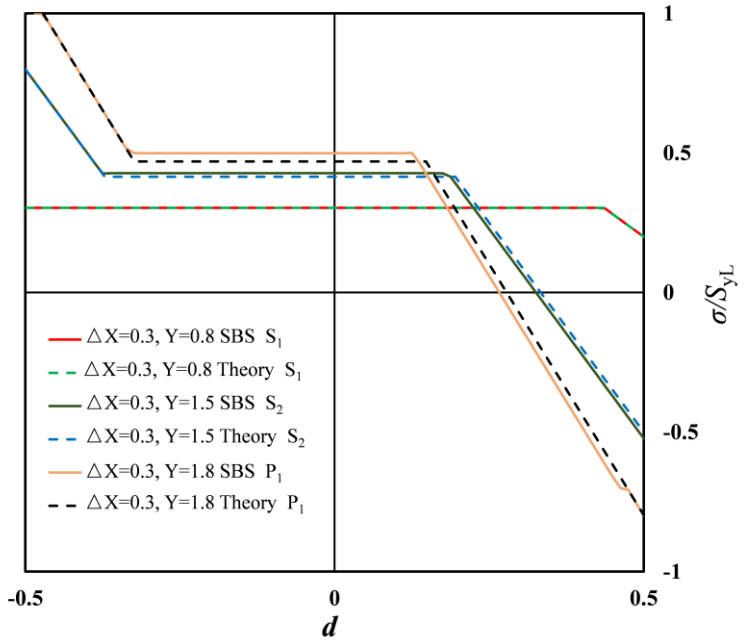

Fig.11. Comparison of numerical and theoretical solutions for elastic core of the out-of-phase loading Bree problem (S_1, S_2, P_1 regions)

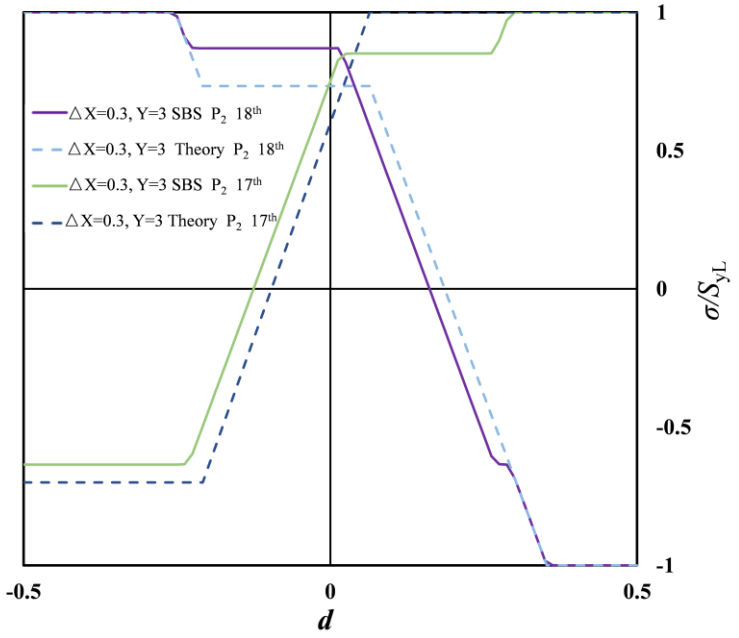

Fig.12. Comparison of numerical and theoretical solutions for elastic core of the out-of-phase loading Bree problem (P_2 region)

5. Discussion on creep ratcheting analysis method under different loading cases

The effective creep stress parameter diagrams (Figs 1, 5 and 10) given in the above three sections assume that the thermal load is a transient condition, that is, the thermal bending stress is caused by the transient temperature gradient during the startup and shutdown of the equipment. In this section, the effective creep stress parameter diagrams under the three types of loading cases are compared, and the conservatism and limitations of the Test B-1 given in ASME NH code are discussed. Then, based on the results in the literature [11], the similarities and differences between the core stress method and another creep ratcheting assessment method which is suitable for sustained thermal load are discussed.

5.1. Discussion on effective creep stress parameter diagram considering different load sequences under transient thermal load condition

Typical Z values are selected in Fig. 13 to compare the equal Z-value lines under classical Bree loading condition and in-phase loading condition. The black line $Z_{\text{Bree}}=1$ is the classical Bree ratcheting boundary, and the dotted line with black dots is the equal Z-value line under Bree loading condition; The green solid line $Z_{\text{in-phase}}=1$ is the Bradford ratcheting boundary, and the green dotted line with red rectangles is the equal Z-value line under in-phase loading condition. Note that the abscissa isΔX for the in-phase loading condition and X for the classical Bree loading. It can be seen that the distribution forms of equal Z-value lines under the two types of loading conditions are the most different in the elastic region and the elastic shakedown region. For the in-phase loading case, there is no core stress in the elastic region, while for the classical Bree loading, the core stress is controlled by primary stress. The ratcheting boundary and equal Z-value lines under the in-phase loading condition are more benign than those under classical Bree loading. Since the equal Z-value line is actually the equal creep life line, the $Z_{\text{in-phase}}$ line encloses a larger safety area compared with the Z_{Bree} line under the same creep life, which means a stronger creep ratcheting resistance. Under the same secondary stress range, the ratcheting boundary and equal Z-value line of the in-phase loading condition have a wider range of primary stress. For example, $Z_{\text{in-phase}}=0.5$ under the in-phase loading condition actually overlaps with a part of the classical Bree ratcheting boundary $Z_{\text{Bree}}=1$.

Fig. 14 selects typical Z values to compare the effective creep stress parameter diagrams under the classical Bree loading and the out-of-phase loading conditions. The black solid lines and the dotted lines with black dots are the results of the classical Bree loading condition, and the blue solid lines and the dotted lines with blue rhombuses correspond to the out-of-phase loading condition. It can be seen that the distribution form of the equal Z-value line under the out-of-phase loading condition is similar to that of the classical Bree loading condition. In the elastic zone E, the equal Z value lines under the two loading conditions are coincident, but the abscissas are actually different. For the elastic shakedown behavior S_1, the equal Z-value lines under the two loading conditions are also coincident, but the S_1 region is smaller for the out-of-phase loading case, as shown in Fig. 1 and Fig.10. In other non-plastic ratcheting regions, the equal Z-value line of classical Bree loading

is more conservative than the corresponding curve of out-of-phase loading case, and the gap between them becomes larger with the increase of Z value.

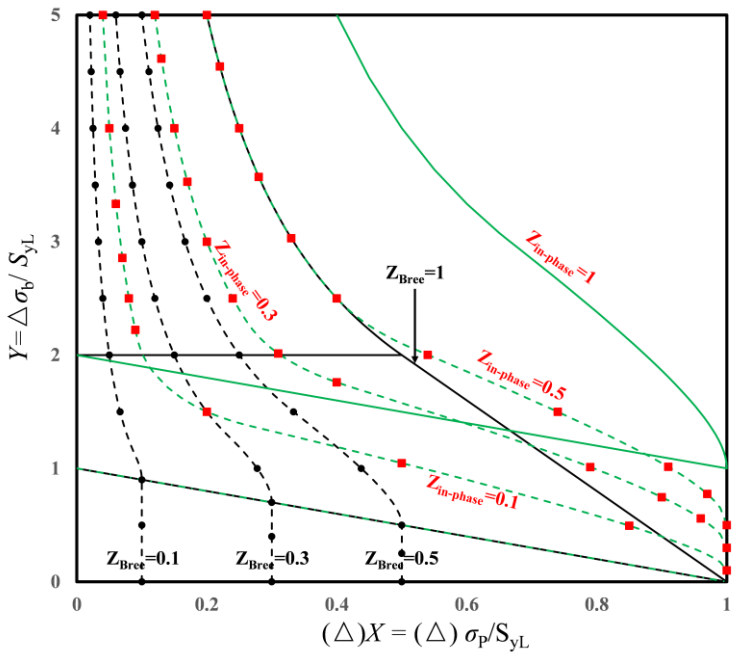

Fig.13. Comparison of effective creep stress parameter diagrams under Bree loading and in-phase loading conditions

The comparison of effective creep stress parameter diagrams under the three loading cases is shown in Fig. 15. It can be concluded that under the same Z-value, the classical Bree loading condition has the most conservative equal Z-value line, followed by the out-of-phase loading condition and the most relaxed in the in-phase loading condition. Therefore, it can be proved that the effective creep stress parameter diagram developed by O 'Donnell and Porowski, although derived from the classical Bree loading, can also be applied to strict in-phase loading and positive out-of-phase loading conditions, i.e., the constant value X can be replaced by the range value ΔX. As can be seen from Fig. 15, it is actually over conservative to use the equal Z-value line under classical Bree loading to approximate the condition of strict in-phase loading. However, strict in-phase loading condition is improbable in actual industrial operation. Compared with the classical Bree loading in which the primary load keeps constant, the out-of-phase loading condition is more common and reasonable considering the cycling of primary load and phase shift between primary and secondary loads. Although it is still conservative to use the equal Z-value line under Bree loading to approximate the corresponding line of out-of-phase loading case, this approximation is convenient and feasible in engineering considering the complexity of the formula of effective creep stress parameters under out-of-phase loading case. The comparison and discussion in this section reveal the conservatism and applicability of the elastic core method under different loading conditions, and provide an important theoretical basis for guiding engineering application and interpreting the code method.

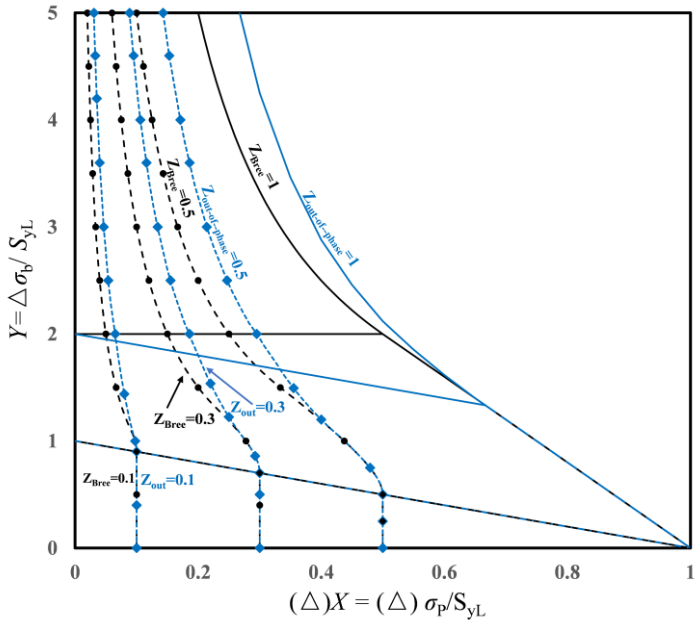

Fig.14. Comparison of effective creep stress parameter diagrams under Bree loading and out-of-phase loading conditions

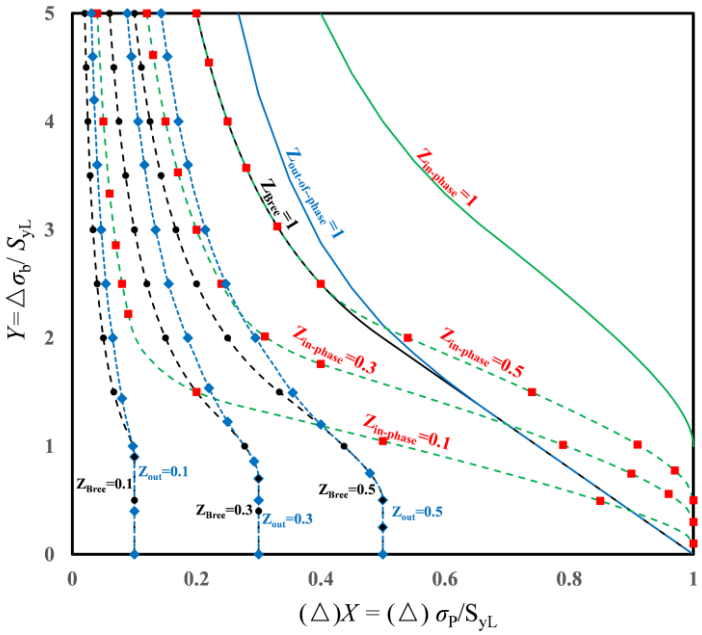

Fig.15. Comparison of effective creep stress parameter diagrams under three loading conditions

5.2. Comparison of creep ratcheting assessment methods under transient thermal load and sustained thermal load conditions

In this section, the elastic core method applicable for transient thermal gradient and another creep ratcheting assessment method applicable for sustained thermal gradient are compared and analyzed under classical Bree loading and in-phase loading conditions. The elastic core method

under the three types of loading conditions discussed above does not actually consider the variation of yield strength with temperature during load cycle, so it is usually suitable for transient thermal load condition. Bradford[11] proposed another creep ratcheting assessment method different from the elastic core method, assuming that the on-load and off-load stages of the Bree problem have different yield strengths. This creep ratcheting assessment method can consider the effect of average temperature during hot end of the cycle on yield stress and applicable to the situation with sustained thermal gradient during steady operation stage. Define the yield strength at the average temperature of the hot end as S_{yH}, and $\alpha=S_{yH}/S_{yL}$. Then, $\alpha=1$ for the elastic core method based on transient thermal gradient, and $\alpha\leq 1$ for Bradford's method based on sustained thermal gradient. Bree considered the influence of average temperature on yield stress in his classic paper[27], but only confined to Bree loading. Bradford[11] reinterpreted the on-load yield stress with creep related physical meaning, and established the creep ratcheting boundaries in detail under the Bree loading and the in-phase loading conditions. The creep ratcheting boundaries under Bree loading are shown in Eqs. (41-43), and the creep ratcheting boundaries under the in-phase loading condition are shown in Eqs. (44-46).

$$XY=\alpha, Y\geq 1+\alpha \tag{41}$$

$$Y=(\sqrt{1-X}+\sqrt{\alpha-X})^2, 1-\alpha\leq Y<1+\alpha \tag{42}$$

$$X=\alpha, 0\leq Y<1-\alpha \tag{43}$$

$$\Delta X\cdot Y=\alpha(\alpha+1), Y\geq 1+2\alpha \tag{44}$$

$$\Delta X+\frac{(Y-1)^2}{4Y}=\alpha, 1\leq Y<1+2\alpha \tag{45}$$

$$\Delta X=\alpha, 0\leq Y<1 \tag{46}$$

By comparing Eqs. (41-43) and (7-9), it can be found that α in Eqs. (41-43) is equivalent to Z in Eqs. (7-9). For Bree loading, when $Z_{Bree}=\alpha_{Bree}$, the equal core stress line applicable to the transient thermal load condition and the creep ratcheting boundary applicable to the sustained thermal load condition coincide. As shown by the green dotted lines in Fig.16. Therefore, the elastic core method under the classical Bree loading condition can be applied to both transient and sustained thermal load conditions. When $Z_{Bree}=\alpha_{Bree}$, the core stress σ_c without the consideration of temperature dependence of yield strength is equivalent to the hot end yield strength S_{yH} with the consideration of temperature dependence of yield strength. Therefore, it can also be considered that the elastic core method of classical Bree problem actually considers the influence of average temperature in high temperature segment on yield strength. The core stress in the non-plastic ratcheting region of the classical Bree diagram must be greater than the constant primary membrane stress σ_p and less than the hot end yield strength S_{yH}, that is, $\sigma_p\leq\sigma_c\leq S_{yH}$. Fig. 16 also shows the creep ratcheting boundaries under in-phase loading condition (red dotted lines) for comparison. Under the same α value, the creep ratcheting boundaries of the two loading conditions are completely coincident in the elastic region. The creep ratcheting boundary under the in-phase loading condition encloses a larger non-creep ratcheting zone than Bree loading condition under the same α value.

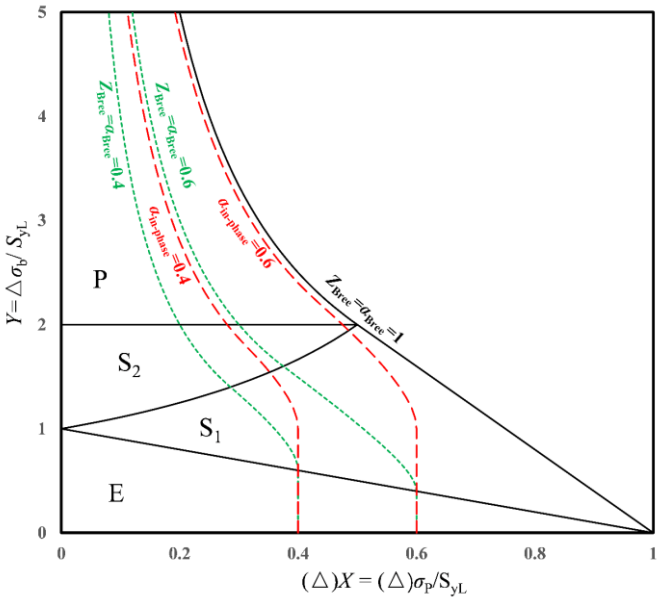

Fig.16. Comparison between equal core stress line and temperature dependent creep ratcheting boundary under Bree loading

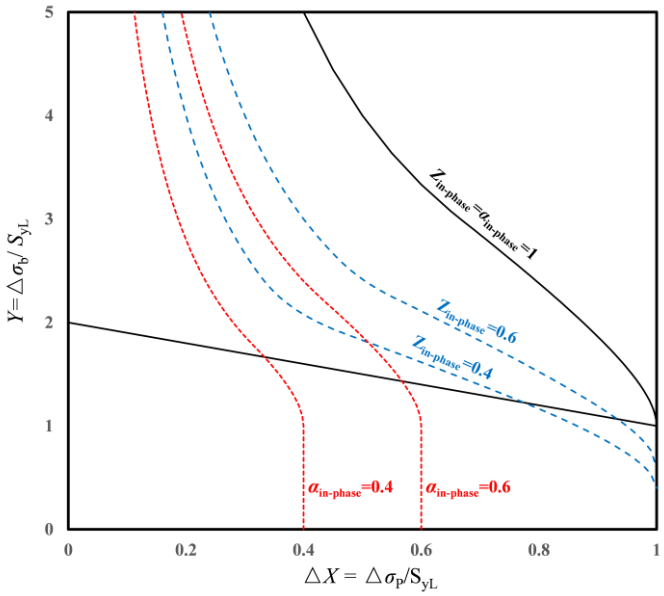

Fig.17. Comparison between equal core stress line and temperature dependent creep ratcheting boundary under in-phase loading

By comparing the formulas (17-22) and (44-46), it can be found that Z and α are not equivalent under the in-phase loading condition. Fig. 17 shows the comparison of the typical equal core stress lines (bule dashed lines marked with Z) and the creep ratcheting boundaries (red dashed lines marked with α) under the in-phase loading condition. It can be seen that there are obvious differences between the core stress line and the creep ratcheting boundary, especially in the elastic shakedown region. Under in-phase loading, the core stress in the elastic zone remains zero, while the creep ratcheting boundary is controlled by the hot end yield strength. When $Z=\alpha$, the creep ratcheting boundary is more conservative due to the consideration of temperature-dependent yield

strength and sustained thermal load. Therefore, for the in-phase loading condition, it is necessary to distinguish whether the thermal load condition (temperature gradient) is transient or sustained.

If the loading sequence of the pressure vessel is divided into four states, namely, startup transient, steady operation, shutdown transient and a period after shutdown, then the loading conditions (Bree loading and in-phase loading) corresponding to the elastic core method and the creep ratcheting boundary are shown in Tables 1-4, where '1' means the load is applied and '0' means the load is removed.

Table 1 Bree loading applicable to elastic core method under transient thermal load

	Startup	Steady operation	Shutdown	After shutdown
P_{max}	1	1	1	1
$\triangle T_{max}$	1	0	1	0

Table 2 In-phase loading applicable to elastic core method under transient thermal load

	Startup	Steady operation	Shutdown	After shutdown
$\triangle P_{max}$	1	0	1	0
$\triangle T_{max}$	1	0	1	0

Table 3 Bree loading applicable to creep ratcheting boundary under sustained thermal load

	Startup	Steady operation	Shutdown	After shutdown
P_{max}	1	1	1	1
$\triangle T_{max}$	1	1	1	0

Table 4 In-phase loading applicable to creep ratcheting boundary under sustained thermal load

	Startup	Steady operation	Shutdown	After shutdown
$\triangle P_{max}$	1	1	1	0
$\triangle T_{max}$	1	1	1	0

6. Conclusions

In this paper, the elastic core concept and effective creep stress parameter diagram of the

modified Bree problems considering in-phase and out-of-phase loading conditions are systematically studied, and two types of creep ratcheting assessment methods under transient and sustained thermal load conditions are discussed. In summary, the key conclusions are as follows:

Compared with the classical Bree loading condition in which the primary stress remains constant, the effective creep stress parameter diagrams considering the cycling of primary stress under the in-phase and positive out-of-phase loading conditions are more benign, that is, the equal core stress line encompasses a wider range of stress parameters. The effective creep stress parameter diagram under strict in-phase loading condition is the most benign, while that under classical Bree loading is the most conservative. Therefore, the Test B-1 of simplified inelastic analysis method in ASME III-1 NH code can be extended directly to the strict in-phase loading condition and positive out-of-phase loading condition, but the constant primary stress X needs to be replaced by the primary stress range ΔX.

For the classical Bree loading condition, the equal core stress line under transient thermal load is equivalent to the creep ratcheting boundary under sustained thermal load. Therefore, the elastic core method is also applicable to the sustained thermal load condition under Bree loading. For the strict in-phase loading case, the equal core stress line is different from the creep ratcheting boundary, and the latter is more conservative.

The results presented in this paper can deepen the understanding of the elastic core concept under generalized loading conditions, and provide guidance for shakedown design and creep ratcheting evaluation of high-temperature components. The new effective creep stress parameter diagrams and formulas have important theoretical significance and engineering value, and can provide reference for the revision and supplement of the integrity design code for components in elevated temperature service.

Acknowledgements

This work is supported by the National Natural Science Foundation of China (12202230, 52150710540) and the Major Project of National Natural Science Foundation of China (12090033).

References

[1] J. Porowski, T. O'Donnell, Elastic Core Concept in Shakedown Analysis, in: ASME Pressure Vessels and Piping Conference, 2008.

[2] W. J. O'donnell, J. Porowski, Upper bounds for accumulated strains due to creep ratcheting, J Pressure Vessel Technol. 96(1974) 150–154.

[3] J. S. Porowski, W. J. O'Donnell, Creep ratcheting bounds from extended elastic core concept, O'Donnell and Associates, Inc., Pittsburgh, PA (USA), 1979.

[4] ASME Boiler & Pressure Vessel Code, III Division 1 NH Class 1 Components in Elevated Temperature Service, Rules for Construction of Nuclear Facility Components, 2013.

[5] R5, Assessment Procedure for the High Temperature Response of Structures, Issue 3 Revision 002, EDF Energy Nuclear Generation Ltd, 2014.

[6] W. J. O'Donnell, J. S. Porowski, M. Badlani, Simplified inelastic analysis methods for bounding fatigue and creep rupture damage, J Pressure Vessel Technol. 102(1980) 394–399.

[7] W. J. O'Donnell, J. S. Porowski, Biaxial model for bounding creep ratchetting in shells, O'Donnell and Associates, 1981.

[8] K.R. Rao, Companion Guide to the ASME Boiler & Pressure Vessel Code, Fourth Edition, Volume 1, (2012), ASME.

[9] W. K. Sartory, Effect of peak thermal strain on simplified ratchetting analysis procedures, Oak Ridge National Lab., 1989.

[10] T. E. McGreevy, F. A. Leckie, P. Carter, et al, The effect of temperature dependent yield strength on upper bounds for creep ratcheting, in: ASME Pressure Vessels and Piping Conference, 2006. 47543: 423-429.

[11] R. A. W. Bradford, J. Ure, H. F. Chen, The Bree problem with different yield stresses on-load and off-load and application to creep ratcheting, Int. J. Pres. Ves. Pip. 113(2014) 32-39.

[12] ASME Boiler & Pressure Vessel Code, Ⅷ Division 2 Alternative Rules, Rules for Construction of Pressure Vessels, 2019.

[13] A. Kalnins, Shakedown Check for Pressure Vessels Using Plastic FEA, ASME-PUBLICATIONS-PVP. 419(2001) 9-16.

[14] A. Kalnins, Shakedown and ratcheting directives of ASME B&PV code and their execution, in: ASME Pressure Vessels and Piping Conference, 2002. 46504: 47-55.

[15] R. A. W. Bradford, The Bree problem with primary load cycling in-phase with the secondary load, Int. J. Pres. Ves. Pip. 99(2012), 44-50.

[16] R. A. W. Bradford, The Bree problem with the primary load cycling out-of-phase with the secondary load, Int. J. Pres. Ves. Pip. 154(2017) 83-94.

[17] X. Pei, P. Dong, A universal approach to ratcheting problems of bree type incorporating arbitrary loading and material nonlinearity conditions, Int. J. Pres. Ves. Pip. 185(2020) 104137.

[18] W. Reinhardt, On the interaction of thermal membrane and thermal bending stress in shakedown analysis, in: ASME Pressure Vessels and Piping Conference, 2008. 48241: 811-822.

[19] R. Adibi-Asl, W. Reinhardt, Ratchet Limit Solution of a Beam With Arbitrary Cross Section, J Pressure Vessel Technol. 137(2015) 031004.

[20] J. Shen, H. Chen, Y. Liu, A new four-dimensional ratcheting boundary: Derivation and numerical validation, Eur. J. Mech. Solid. 71(2018) 101-112.

[21] H. Bao, J. Shen, Y. Liu, et al, Shakedown analysis of modified Bree problems involving thermal membrane stress and generalized loading conditions, Int. J. Pres. Ves. Pip. 192(2021) 104432.

[22] H. Bao, J. Shen, Y. Liu, et al, Shakedown analysis and assessment method of four-stress parameters Bree-type problems, Int J Mech Sci. 229(2022) 107518.

[23] D. Moreton, H. Ng, The extension and verification of the Bree diagram, in: Structural Mechanics in Reactor Technology, L, 1981.

[24] H. W. Ng, D. N. Moreton, Alternating plasticity at the surfaces of a Bree cylinder subjected to in-phase and out-of-phase loading, J Strain Anal Eng. 22(1987) 107–113.

[25] H. W. Ng, D. N. Moreton, Ratchetting rates for a Bree cylinder subjected to in-phase and out-of-phase loading, J Strain Anal Eng. 21(1986) 1–7.

[26] D. W. Spring, C. Panzarella, D. A. Osage, Revisiting the bree diagram, in: ASME Pressure Vessels and Piping Conference, 2016.

[27] J. Bree, Elastic-plastic behavior of thin tubes subjected to internal pressure and intermittent high-heat fluxes with application to fast-nuclear-reactor fuel elements, J. Strain Anal. 2 (3) (1967) 226–238.